Measurement system for monitoring of vibrations in mechanical devices

Wacław Gawędzki, Zbigniew Marszałek

AGH University of Science and Technology, Faculty of Electrical Engineering, Automatics, Computer Science and Biomedical Engineering, Krakow

Abstract: The ongoing assessment of the technical state of selected mechanical devices requires the use of systems which monitor their operating parameters. As an example, one of the key elements of mechanical devices are bearings, and an important indicator allowing for the assessment of their technical state are the absolute vibration acceleration values for the bearing housing. In the article, we discuss the construction of a system allowing for the monitoring of vibration acceleration signals in mechanical devices using a 3-axial system. In this article, we propose more complex methods of analysis and compare them in terms of effectiveness of assessment of the technical state of the tested device with the methods currently in use. For this reason, for the analysis of vibration signals we used two additional methods based on short-time Fourier transformation (STFT) and Hilbert–Huang transformation (HHT). For all methods, both those used traditionally and those now being proposed, we defined criteria and compared their sensitivity in terms of the assessment of the technical state of the tested object, using the example of a slide bearing.

Keywords: monitoring, bearing, vibration, Fourier transformation, Hilbert–Huang transformation

SYSTEM POMIAROWY DO MONITORINGU DRGAŃ URZĄDZEŃ MECHANICZNYCH

Streszczenie: Bieżąca ocena stanu technicznego wybranych elementów urządzeń mechanicznych wymaga zastosowania systemu monitoringu ich parametrów pracy. Na przykład jednym z istotnych elementów urządzeń mechanicznych są łożyska, a ważnym wskaźnikiem umożliwiającym ocenę ich stanu technicznego są wartości przyspieszeń drgań bezwzględnych obudowy łożyska. W artykule omówiono budowę systemu pomiarowego umożliwiającego monitoring sygnałów przyspieszeń drgań urządzeń mechanicznych w układzie trójosiowym. W artykule zaproponowano bardziej zaawansowane metody analizy i porównano je pod kątem skuteczności oceny stanu technicznego badanego urządzenia z metodami aktualnie stosowanymi. Do analizy sygnałów drgań zastosowano w związku z tym dwie dodatkowe metody bazujące na krótkoczasowej transformacji Fouriera STFT i transformacji Hilberta–Huanga HHT. Dla wszystkich metod, klasycznie stosowanych i proponowanych, zdefiniowano kryteria oraz porównano ich wrażliwość pod względem oceny stanu technicznego badanego obiektu, na przykładzie łożyska ślizgowego.

Słowa kluczowe: monitoring, łożysko, drgania, transformacja Fouriera, transformacja Hilberta–Huanga

https://doi.org/10.7494/978-83-66727-47-2_4

1. Introduction

Assessing the technical condition of selected elements of mechanical and electromechanical devices, machines or drive systems requires a dedicated system to monitor their operating parameters. Depending on the type of device, these parameters can include e.g.: torque, rotational speed, temperature, axial and radial displacements as well as relative and absolute vibration. For example, bearings are an important component of mechanical devices, and the absolute vibration acceleration values of their housing allow their technical condition to be assessed (Lepiarczyk and Gawędzki 2018). The search for new diagnostic systems is particularly important in the case of drive systems whose rotational movement generates vibrations and whose acceleration values depend on the condition of the bearings (Cioch et al. 2013). Frequently, analysis of acoustic signals generated by the mechanical device is used for diagnostic purposes. The values of acoustic parameters are measured, e.g. sound pressure level and saturation level (Borghesani et al. 2018, Poddar and Tandon 2019).

The simplest used diagnostic systems mainly measure basic parameters of the vibroacoustic signal in the time domain, such as: vibration RMS value, maximum value, peak-to-peak value, power and energy of the signal etc. (Yang and Kim 2004, Lepiarczyk and Gawędzki 2018). Statistical methods, on the other hand, are based on the determination of predicted values, standard deviations, variances, correlations, moments, etc. Also used are stochastic methods, probability distributions, as well as identification of changes in signal character involving change point detection (Poulimenos and Fassois 2006, Obuchowski et al. 2013). Among the interesting methods used are also diagnostic methods based on the use of time series for modelling vibration signals in changing operating conditions. Due to the fact that these signals have modulating amplitude and frequency values (time-varying spectrum), ARMA models are used with time-varying model coefficients (Wyłomańska et al. 2014).

Analysis of vibroacoustic signals in the domain of frequency is carried out by using Fourier transform, and as a result a spectrum distribution is obtained which provides information on the harmonics occurring in the signal and their amplitudes and frequencies (Yang and Kim 2004, Obuchowski et al. 2014a, Lepiarczyk and Gawędzki 2018). A further development in diagnostic methods in the domain of frequency are time-frequency transforms, which are particularly applicable in cases of non-stationary vibration phenomena (Obuchowski et al. 2014b). These include, for example, continuous wavelet transform (Tse et al. 2004) and STFT (short-time Fourier transform).

The monitoring of vibration is conducted not only with regard to machinery and electromechanical devices. Other objects are also monitored, including buildings, linear constructions (gas and oil pipelines), mining structures and buildings in the vicinity of mining areas and transportation channels, bridges, and viaducts. In the course of

this monitoring, the data sets collected are large, leading to difficulties in their analysis. For this reason, mechanisms are being introduced into the on-baord programming of this equipment for the automatic analysis of data based on Machine Learning, which use AI to analyse the data.

A typical vibration monitoring system includes a measurement transducer (such as an accelerometer or vibrometer), an amplifier, a signal acquisition system, and software for the measurement system, most often involving analysis of the measured data. The selection of the appropriate sensor depends on the range of measured values of vibration parameters, their amplitudes and frequency bands. In the case of measurement of high-frequency vibrations (in machinery and electromechanical devices), vibration acceleration is measured using piezoelectric accelerometers in items with load output or built-in IEPE (integrated electronics piezo electric) amplifiers (B&K 2016). Each of these sensors requires a different type of amplifier to condition the signal. In the case of analysis of low-frequency vibrations (buildings and construction sites, vibration of the rock mass in mining), the displacement or velocity of vibration is measured using a vibrometer, while in mining itself, geophones are used. While dedicated amplifiers are required for work with sensors, acquisition systems most often are of a universal nature, being for example measurement cards with appropriately selected metrological parameters. The software used in the measuring system, and in particular the methods of data analysis applied, are adapted to the particular type of object being monitored and to the aim of the monitoring.

This article focuses on more complex methods of analysis and compares their effectiveness in assessing the technical condition of the tested devices with those currently in use. Methods presented in Figure 1 were used to analyse the vibration signals in the time domain, frequency domain (Fourier transform (FT)), and time-frequency domain (short-time Fourier transform (STFT) and Hilbert–Huang transform (HHT) (Huang et al. 1998).

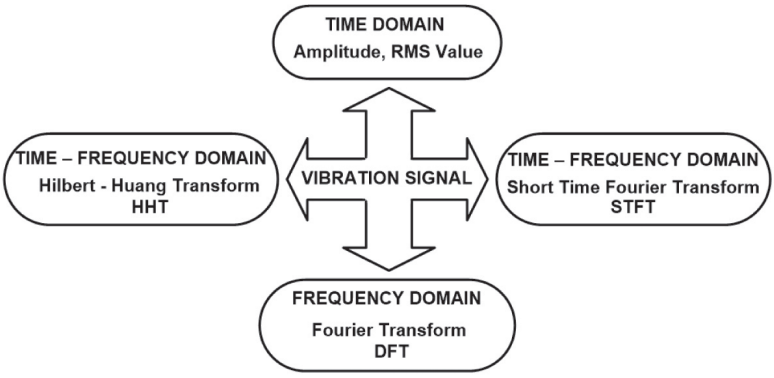

Fig. 1. Methods of analysing vibration signals in the time domain, DFT frequency domain as well as STFT and HHT time-frequency domain

Each of the transformations has different properties, especially when it comes to their application in analysing non-linear and non-stationary phenomena. In the monitoring system, measurements were taken cyclically with a specific time interval. In each measurement cycle, sequences of signal values with a specific number of samples and duration were recorded.

When applying the method to analysis in the time domain, the RMS values of vibration acceleration were determined for each of the recorded signal sequences. A change in RMS values is indicative of changes in bearing operation depending on its technical condition and load.

The second method used was frequency analysis using the FT. Firstly, this type of analysis allows, among other things, the distribution of amplitudes and RMS values of sinusoidal components of vibration signals to be determined for the frequency values occurring in the analysed signal, assuming the stationary nature of the phenomena. Secondly, it also allows the resonance properties of mechanical systems to be identified. Finally, it is also possible to obtain information on phase relationships between individual components, which can be used in system diagnostics.

In the third and fourth approach, the methods of time-frequency analysis using STFT and HHT were applied. Both methods are well suited to analysing phenomena of a non-stationary character, and in the case of HHT also of a non-linear character. The STFT method allows the amplitude distribution and RMS values of vibration signal sinusoidal components to be determined for frequency values occurring in the analysed signal, taking into account a potential change in time function.

The HHT transformation consists of two stages (Huang 1998, Feldman 2011, Gawędzki and Serzysko 2015, Gawędzki 2016). First, the empirical mode decomposition (EMD) algorithm decomposes the signal to narrowband intrinsic mode function (IMF) components from highest to lowest frequency. Then, the EMD algorithm is complemented by the Hilbert transformation, which allows the values of momentary frequencies, amplitudes and RMS of the signal's IMF components decomposed by the EMD algorithm to be determined.

The article shows how the presented methods can be used to analyse vibration signals using the slide bearing pan as an example. The construction of a measurement system which allows vibration acceleration signals to be continuously monitored in a 3-axis system is discussed. During testing, the sensitivity of various proposed methods of vibration signal analysis to forced changes in the bearing load was examined

2. Theory of vibration process modelling

In the monitoring system, the measurements of the slide bearing vibration acceleration in the drive unit were performed continuously in a 3-axis system. The measure-

ment results were recorded cyclically, with a pre-set time interval of Θ. In each cycle, sequences of signal values with a specific number of N samples were recorded with a sampling frequency of fs, so the duration of a single recording cycle T was equal to:

$$T = \frac{N}{f_s} \tag{1}$$

where $T < \Theta$.

The temporal values of vibration acceleration signals do not directly provide diagnostic information about the system. Therefore, in order to find a criterion which would return definite diagnostic information, additional tests were carried out. For this purpose, the following parameters of vibration acceleration signals were analysed: time, frequency FT, time-frequency STFT and HHT (Huang 1998, Feldman 2011). The criteria were defined and their effectiveness in assessing the technical condition of the examined object was compared.

When analysing discrete time, the I_1 norm of the vector of recorded data $a[n]$ in the form of (Turowicz 2005) was used as the criterion:

$$I_1 = a[n] = \sqrt{\frac{1}{N}\sum_{n=0}^{N-1} a^2[n]} \tag{2}$$

where $a[n]$ – the vector of N recorded vibration acceleration samples.

This criterion corresponds to the RMS value of vibration acceleration determined for time T for recorded signal sequences in each of the three axes. It has a physical sense of the element from the average signal power in the range of [0÷N-1] (the range corresponds to time T, in which N samples with sampling frequency f_s were recorded).

The second method used was a frequency analysis using the discrete Fourier DFT transformation. It allows the distribution of amplitudes of sinusoidal components of vibration signals to be determined for frequency values occurring in the analysed signal, assuming the stationary character of the occurring phenomena. The application of the DFT allows the combined frequency spectrum $A[k]$ of acceleration signals to be determined, which takes the form of (Oppenheim and Schafer 1999):

$$A[k] = \mathrm{DFT}\{a[n]\}, \quad k = 0, 1, 2, ..., N-1 \tag{3}$$

where:

N – number of frequency bands of the signal,
k – number of the spectrum band.

The relevant information is stored in the first $N/2+1$ bands, whose frequency value is equal to:

$$f_k = k\frac{f_s}{N}, \quad k = 0, 1, 2, ..., \frac{N}{2} \tag{4}$$

After scaling $A[k]$ (3), the RMS value of the vibration acceleration of the k component $\tilde{A}[k]$ of the spectrum is equal to:

$$\tilde{A}[k] = \frac{2}{N\sqrt{2}}\left|A[k]\right|, \quad k = 0, 1, 2, ..., \frac{N}{2} \tag{5}$$

When conducting the analysis using the FT for frequency, the I_2 vector $\tilde{A}[k]$ norm in the form of (Turowicz 2005) was used as the diagnostic criterion:

$$I_2 = \tilde{A}[k] = \max_{0 \le k \le \frac{N}{2}} \left|\tilde{A}[k]\right| \tag{6}$$

where the k argument for the band number meets the condition:

$$k = \arg\max\left|\tilde{A}[k]\right| \tag{7}$$

for which the frequency is determined by (4). The value of criterion I_2 corresponds to the RMS value of the vibration acceleration determined for time T, for each of the three measuring axes of the accelerometer.

In the third approach, the method of time-frequency analysis using STFT was used. This transformation is well suited for analysing non-stationary phenomena. It allows the amplitude distribution of sinusoidal components of vibration signals to be determined for frequency values occurring in the analysed signal, taking into account their possible change as a function of time. The $A[n, k]$ spectrum of vibration acceleration signals, determined by means of a discrete STDFT transformer, takes the form of (Oppenheim and Schafer 1999):

$$A[rR,k] = \sum_{m=0}^{L-1} a[rR+m]w[m]e^{-j\left(\frac{2\pi}{N}\right)km}, \quad k = 0, 1, 2, ..., N-1 \tag{8}$$

where:

$a[n]$ – vector of recorded N samples of vibration acceleration,
$w[m]$ – time window with a length of L,
N – number of signal samples for frequency as well as length of the DFT transformer,
k – number of the spectrum band (frequency corresponding to the band according to (4)), where relevant information is stored in the first $N/2+1$ bands,
R – width of the sampling interval of the transformer for time,
r – number of the transformer sample for time.

In general, the transformer parameters (8) should meet the condition:

$$N \geq L \geq R \tag{9}$$

After scaling $A[rR, k]$ (8), the RMS value of the vibration acceleration of the k component $\tilde{A}[rR, k]$ of the spectrum is equal to:

$$\left(\tilde{A}\right)[rR,k] = \frac{2}{N\sqrt{2}}\left|A[rR,k]\right|, \quad k = 0, 1, 2, ..., \frac{N}{2} \tag{10}$$

For the STFT in the discrete STDFT version, a diagnostic criterion in the form of the I_3 norm of the $\tilde{A}[rR, k]$ matrix was used (Turowicz 2005):

$$I_3 = \tilde{A}[rR,k] = \max_{0 \leq r \leq \frac{N-L}{R}+1} \max_{0 \leq k \leq \frac{N}{2}} \left|\tilde{A}[rR,k]\right| \tag{11}$$

where the k argument for the band number meets the condition:

$$(r,k) = \arg\max \left|\tilde{A}[rR,k]\right| \tag{12}$$

for which the frequency is determined by (4).

In the fourth approach, the method of decomposing the vibration acceleration signal in the time domain using the HHT was applied. This method is well suited for analysing phenomena of a non-stationary character, including non-linear ones. The HHT method allows the distribution of amplitudes of sinusoidal components of vibration signals to be determined for frequency values occurring in the analysed signal, taking into account their possible change in the time function.

The HHT consists of two stages (Huang 1998, Gawędzki 2016). In the first stage, the EMD algorithm decomposes the signal into narrowband IMF components from highest to lowest frequency. In the second stage, the narrowband components of the IMF are transformed by the Hilbert transformation. This allows the values of momentary amplitudes and frequencies of EMD-decomposed IMF components of the signal to be determined.

The principle of the EMD algorithm is based on iterative separation of the subsequent functions of the IMF components: $a_1[n]$, $a_2[n]$, ..., $a_N[n]$ and the residual signal $r_K[n]$ from the primary signal $a[n]$, so that the equation is finally met:

$$a[n] = \sum_{i=1}^{K} a_i[n] + r_K[n] \tag{13}$$

The EMD algorithm is described in detail in Huang (1998), Feldman (2011), Gawędzki and Serzysko (2015). In the second stage of the HHT, each i-th component

of the IMF $a_i[n]$ is described by slow-change functions of discrete time: amplitudes $A_i[n]$ and phase $\Phi_i[n]$:

$$a_i[n] = A_i[n]\cos\Phi_i[n] \quad \text{for} \quad i = 1, 2, ..., K \tag{14}$$

As a result of the decomposition of each acceleration signal $a[n]$, we obtain K-components in decreasing frequency order, but only some of them carry significant energy value. The RMS value $\tilde{A}_i$ of acceleration of vibrations of i-th component $A_i[n]$ of the spectrum (13) is determined from the relation:

$$\tilde{A}_i = \sqrt{\frac{1}{N}\sum_{n=0}^{N-1} A_i^2[n]} \quad \text{for} \quad i = 1, 2, ..., K \tag{15}$$

The I_4 vector $\tilde{A}_i$ (14) norm in the form of (Turowicz 2005) was used as the diagnostic criterion for using time domain acceleration signal decomposition:

$$I_4 = \tilde{A}_i = \max_{1\le i\le K}\left|\tilde{A}_i\right| \tag{16}$$

where the i argument, which determines the number of the IMF component, meets the condition:

$$i = \arg\max\left|\tilde{A}_i\right| \tag{17}$$

For the sensitivity analysis of diagnostic criteria $I_1 \div I_4$ to the change of vibration acceleration forced by the increase of the load on the tested bearing, the following measure was proposed:

$$\Delta_n = I_n(t_m + \Theta) - I_n(t_m) \quad n = 1 \div 4 \tag{18}$$

where:

t_m – the moment of time when the forced m-change of the load takes place,
Θ – the interval of time during which successive sequences of signal values are cumulatively recorded, the duration of a single sequence being T (1).

The values of criteria $I_1 \div I_4$ and criterion Δ_n (18) are to be determined for each axis X, Y and Z, in which the acceleration values are measured, as well as for all moments of time t_m in which load change occurs.

3. Vibration acceleration measurement system

The measurement system was built on the basis of an 8-channel Spider8 measurement card from Hottinger Baldwin Messtechnik (Fig. 2) (HBM 2003). This is an exter-

nal card integrated by means of a USB interface. It has measurement channels equipped with separate A/D converters and anti-aliasing filters with a programmable limit frequency and Bessel or Butterworth filter types. The measurement channels enable the integration of sensors with voltage, current, resistive, and bridge output in full and half bridge configurations. They also have functions that allow direct connection and temperature measurement using typical thermoelectric and thermoresistive sensors.

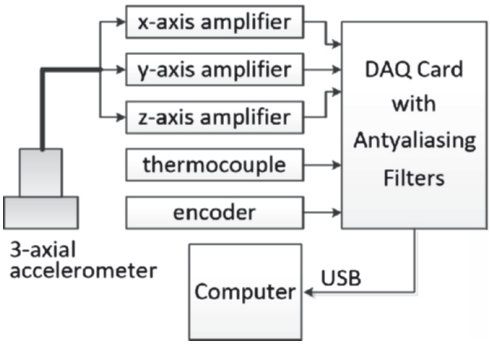

Fig. 2. Diagram of the vibration measurement system with computerised signal analysis

To measure the vibration acceleration, a 3-axis type 4528-B-001 piezoelectric accelerometer in CCLD technology from Brüel & Kjær (B&K 2016) was used, which worked with dedicated load amplifiers with type 1704-A-001 voltage outputs. The measuring range of the accelerometer is 70 m/s^2 in the frequency band from 0.3 Hz to 12,800 Hz. By appropriately selecting the settings of the amplifiers, the measurement range of acceleration measurement channels in each axis was set to 10 m/s^2. An optical converter was used to measure the speed. The measurement range of the encoder was 3000 rpm with a measurement resolution of 1/360 rpm. The temperature of the slide bearing housing, in the immediate vicinity of the shaft pin, was measured by means of a K-type thermoelectric needle thermometer, placed in a hole made in the housing.

A computer controls the measurement system using HBM Catman software. The computer implements the algorithms of signal processing and determination of the values of the diagnostic criteria $I_1 \div I_4$ and the criterion of evaluation of their sensitivity Δ_n (18) discussed in Section 2.

4. A sample tested object

Figure 3 shows a block diagram of the measuring station, while Figure 4 shows a photograph, as an example, of a tested slide bearing with measuring sensors (Lepiarczyk 2015, Lepiarczyk and Gawędzki 2018).

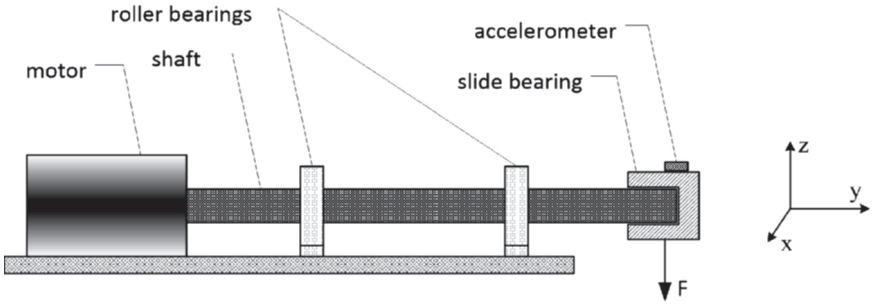

Fig. 3. Block diagram of the measuring station

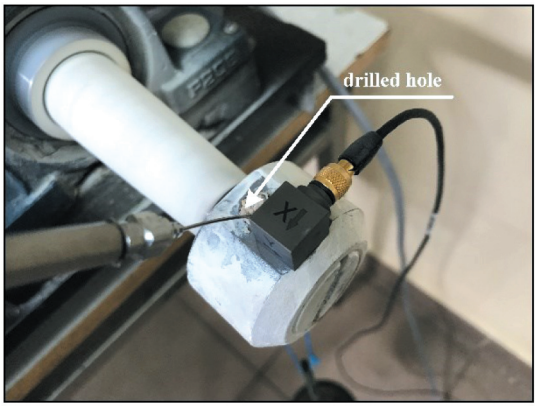

Fig. 4. View of slide bearing with measuring sensors
Source: Lepiarczyk and Gawędzki (2018)

The inverter-controlled motor drives the bearing shaft with two roller bearings. The transverse load was applied with a force of F to the slide bearing node by means of weights attached to the slide bearing pan. During testing, the slide bearing was loaded with a gradually increasing force of F. Measurements of vibrations of the slide bearing node were carried out by means of a 3-axis accelerometer. The accelerometer was fixed to the pan with a screw.

Temperature control of the slide bearing node was performed by means of a needle thermocouple fixed in a specially drilled hole in the pan (Fig. 4). The solution used made it possible to measure the operating temperature of the slide bearing near the contact of the rotating shaft pivot in the pan of the tested slide bearing.

5. The experiment

The slide bearing was tested in lab conditions. The operation of the bearing was tested at a fixed speed. The experiments were carried out in such a way that in the first

stage, the system worked with the bearing pan on the pin of the shaft and the preload $F_0 = 12.45$ N applied at half the width of the pan housing, perpendicular to the axis of the bearing (Fig. 3).

In this way, the bearing operated under load until its temperature stabilised. Then at $t_1 = 60$ min (18), the load was increased to $F_1 = 22.26$ N and, similarly as in the previous stage, the measurement was taken up to the point when the temperature stabilised at increased load. The action was repeated, increasing successively in stage 2, at $t_2 = 90$ min increasing the load to $F_2 = 32.07$ N and in stage 3, at $t_3 = 120$ min to $F_3 = 41.87$ N.

The measurements were planned to be made in the frequency range correlating to the shaft speed. For the experimental speed of $n = 1496$ rpm, the frequencies are 24.9 Hz and its higher harmonics were used. The sampling and limiting frequencies of the filter were selected with respect to the processes being studied. A sampling frequency of the measurement system $fs = 600$ Hz (1) with an anti-aliasing filter with a limiting frequency of 150 Hz was assumed.

Measurements were taken in a continuous manner with cyclic recording of measurement results every 5 min ($\Theta = 5$ min (1)) for a bearing lubricated with SN100 oil, using a 3-axis piezoelectric accelerometer. The selection of a 1-minute resolution in the analysis of vibration of a given object was determined by the dynamics of the processes occuring within the object. During each recording, 20-second ($T = 20$ s) sequences of acceleration signals were recorded. The total measurement time was 150 minutes and 31 recorded sequences of measurement signals were obtained. During the experiment, the load on the slide bearing was increased. For each registered 20-second sequence of vibration signals of the slide bearing, the values of criteria $I_1 \div I_4$ were determined according to (2), (6), (11) and (16) and their sensitivity measures $\Delta_1 \div \Delta_4$ according to (18).

6. Results

On the basis of the measurement experiments conducted, the analysis of recorded sequences of vibration acceleration signals was carried out and the values of criteria $I_1 \div I_4$ were determined. Figures 5–8 show the changes in the values of the criteria determined as a function of time for the selected X-axis, for example (Fig. 3). The choice of this axis is due to the fact that the vibration accelerations in the X-axis reached their highest values. The points on the diagrams marked with circles determine the time moments of the cyclic recording of signal sequences with a time interval of 5 min.

The value corresponding to each point determines the value of the criterion determined on the basis of a recorded 20-second sequence of vibration signals, starting at a given point in time. Three arrows on each graph indicate the moments of time when the load on the tested bearing was increased in subsequent stages of the experiment. The values of the forces and the moments of time at which they were applied are shown in Table 1.

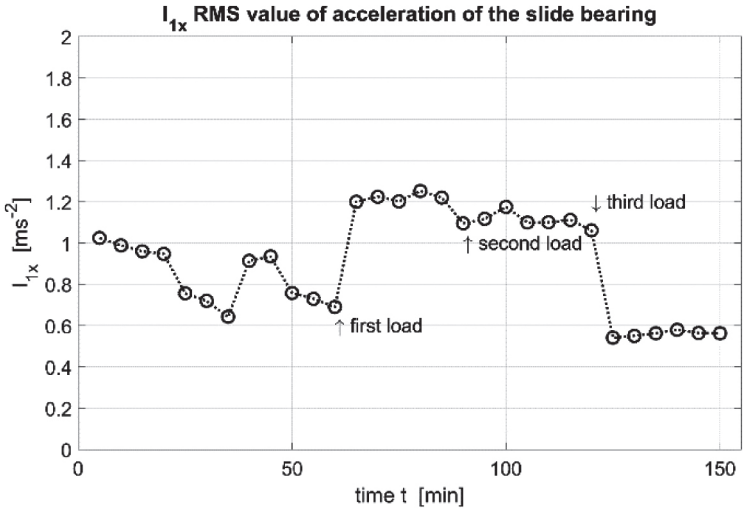

Fig. 5. Running criterion I_1 of the RMS value of bearing vibration acceleration in the X-axis as a function of time, according to (2)

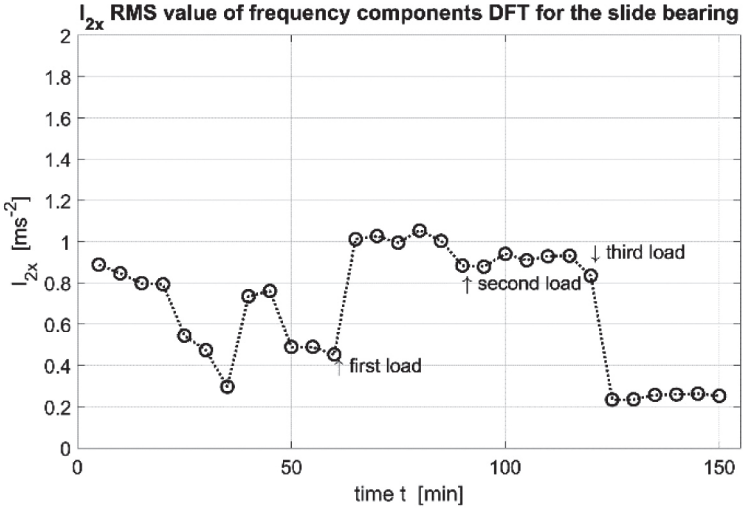

Fig. 6. Running criterion I_2 of the RMS value of the DFT component of the bearing vibration acceleration in the X-axis as a function of time, according to (6)

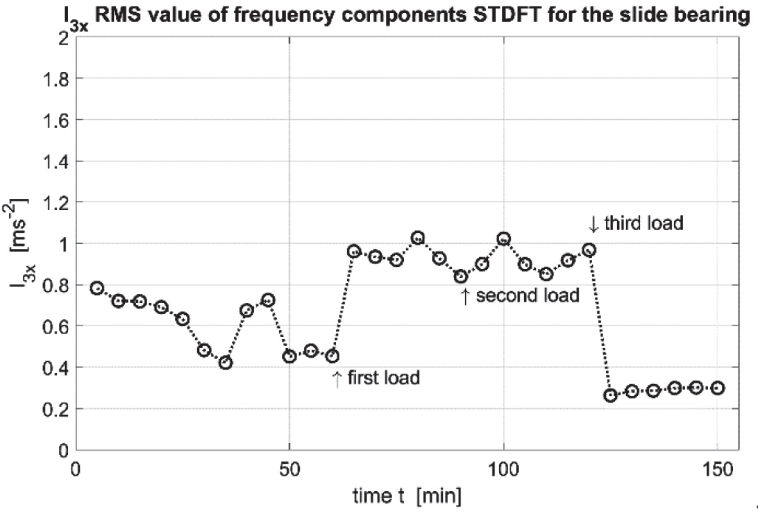

Fig. 7. Running criterion I_3 of the RMS value of the STFT component of the bearing vibration acceleration in the X-axis as a function of time, according to (11)

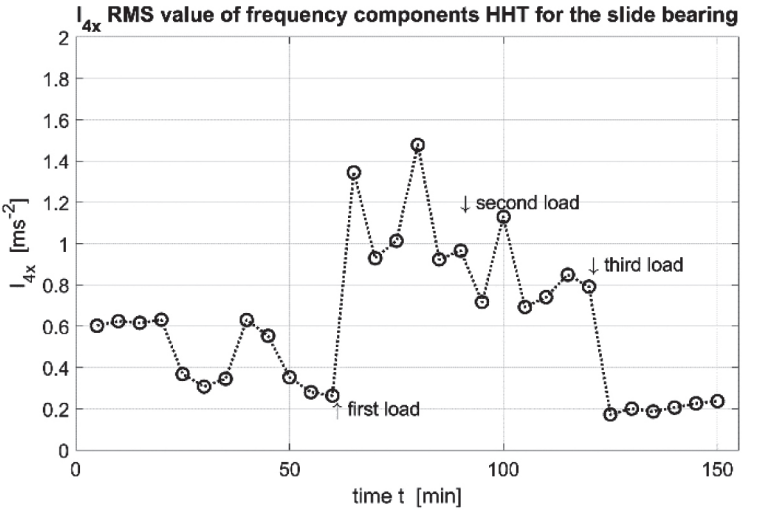

Fig. 8. Running criterion I_4 of the RMS value of the HHT component of the bearing vibration acceleration in the X-axis as a function of time, according to (16)

Table 1
Summary of the moments of time when the bearing load was increased

Time [min]	$t_1 = 60$	$t_2 = 90$	$t_3 = 120$
Force [N]	$F_1 = 22.26$	$F_2 = 32.07$	$F_2 = 41.87$

The analysis of the recorded results of the acceleration measurements was carried out on the basis of the determined RMS values of the vibration acceleration of the bearing pan, measured along the X, Y and Z axes. The RMS values were determined by different methods: in the time domain (according to (2)), in the frequency domain for spectral components based on DFT (according to (6)), and in the time and frequency domain also for spectral components based on STFT (according to (11)) and HHT (according to (16)). The highest acceleration values were obtained for measurements in the X-axis, in the direction perpendicular to the shaft axis and to the direction of earth acceleration (the direction of the X-axis is shown in Figure 3).

The results obtained by the mentioned methods for the X-axis, shown in Figures 5–8, illustrate the changes in the RMS values of vibrations over 150 minutes, with increasing bearing load. The graphs clearly show the change in the RMS values of the vibration acceleration immediately after the load change. A similar phenomenon occurs for the Y and Z axes, but the changes in the acceleration values are smaller. The variability of the recorded vibration signal during the first 60 min of the experiment, which can be seen in Figures 5–8, is a result of the process of the settling of operating conditions in the bearing (warm-up, increase in temperature, until a working temperature is reached). Subsequent vibration signal variability after the lapse of 60 min results from the increased load on the bearing, lasting until the end of the experiment. This was because each increase in the load was accompanied by an increase in temperature and the associated change in operating conditions. It should be clearly emphasised here that the variability recorded in this experiment is not of a universal nature, but rather is related to the individual characteristics of the studied bearing. Conversely, the significant change in the values of recorded signals immediately after the change in load on the bearing is of a universal nature.

Based on the relation (4), it is also possible to determine the values of the dominant frequencies in the vibration spectrum for the DFT frequency method as well as STFT and HHT time-frequency methods for the k-band for which the maximum RMS value of the vibration accelerations is achieved in each method.

For the purposes of quantitative evaluation and comparison of the effectiveness of diagnostic criteria $I_1 \div I_4$, a measure of sensitivity Δ_n (according to (18)) to change of vibration accelerations caused by increasing load on the tested slide bearing was defined. Table 2 shows the values of sensitivity measures $\Delta_1 \div \Delta_4$ for all axes X, Y and Z, determined according to (18), for diagnostic criteria $I_1 \div I_4$, at different values of slide bearing load forces $F_1 \div F_3$. To better illustrate the numerical values in Table 2, they are also shown in graphical form on the diagrams in Figures 9–11. Each of the diagrams, respectively for the x, y and z axes, shows the sensitivity measures $\Delta_1 \div \Delta_4$ for all four criteria $I_1 \div I_4$. These take into account the distribution of the values of sensitivity measures depending on the load force F of the tested slide bearing.

Negative values of the sensitivity measures apply when the RMS value of the vibration acceleration decreases (18). The sensitivity of the fourth criterion I_4 is clearly the highest in the X-axis (Fig. 9), and not lower than the other values of the criteria in the Y-axis (Fig. 10). In the Z-axis, on the other hand (Fig. 11), due to the very small values of vibration acceleration, it is not possible to determine whether the presented hierarchy of sensitivity measures is correct and does not result, for example, from measurement errors or interference. Comparing the figures in Table 2, it can be seen that criteria I_1 and I_4 show greater sensitivity than criteria I_2 and I_3.

Table 2
Values of sensitivity measures $\Delta_1 \div \Delta_4$ (18) of the diagnostic criteria $I_1 \div I_4$ for different values of slide bearing load forces $F_1 \div F_3$

Load force [N]		Δ_1 [m/s^2]	Δ_2 [m/s^2]	Δ_3 [m/s^2]	Δ_4 [m/s^2]
X-axis	$F_1 = 22.26$	0.510	0.560	0.508	1.082
	$F_2 = 32.07$	0.021	–0.004	0.060	–0.249
	$F_3 = 41.87$	–0.520	–0.600	–0.705	–0.620
Y-axis	$F_1 = 22.26$	–0.274	–0.008	–0.006	0.255
	$F_2 = 32.07$	0.083	0.070	0.062	–0.419
	$F_3 = 41.87$	0.135	0.122	0.096	0.139
Z-axis	$F_1 = 22.26$	0.005	–0.060	–0.024	–0.014
	$F_2 = 32.07$	0.205	0.230	0.118	0.079
	$F_3 = 41.87$	–0.018	–0.059	–0.077	0.028

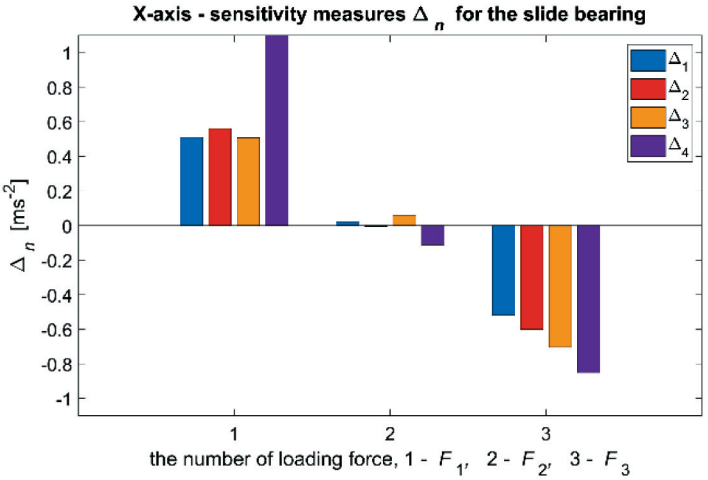

Fig. 9. Summary of sensitivity measure values $\Delta_1 \div \Delta_4$ of diagnostic criteria $I_1 \div I_4$ to change of vibration acceleration in the X-axis, caused by increasing load of the tested slide bearing

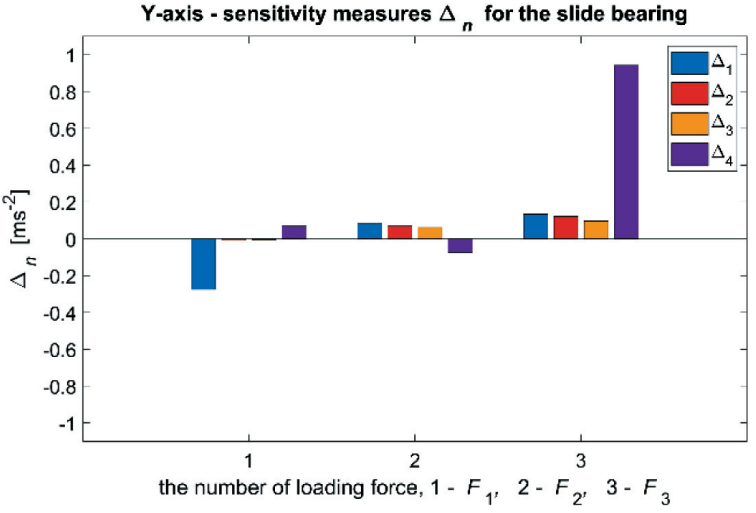

Fig. 10. Summary of sensitivity measure values $\Delta_1 \div \Delta_4$ of diagnostic criteria $I_1 \div I_4$ to change of vibration acceleration in the Y-axis, caused by increasing load on the tested slide bearing

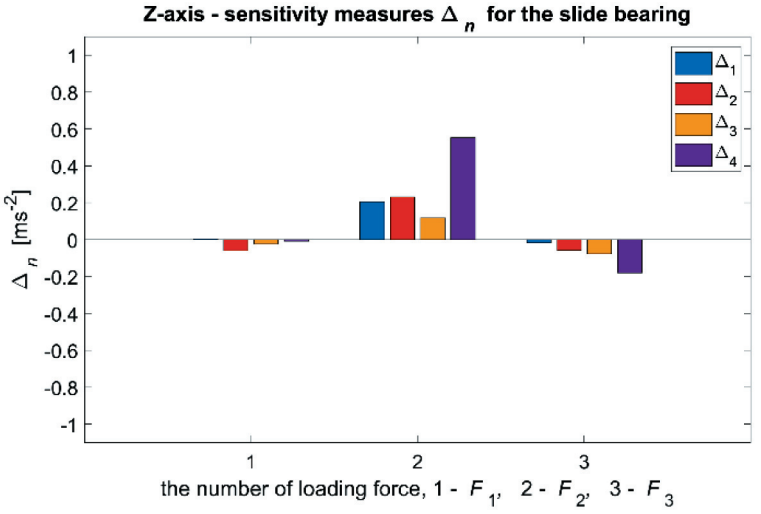

Fig. 11. Summary of sensitivity measure values $\Delta_1 \div \Delta_4$ of diagnostic criteria $I_1 \div I_4$ to change of vibration acceleration in the Z-axis, caused by increasing load of the tested slide bearing

7. Conclusions

The results of the analysis of the recorded vibration acceleration signals confirmed the effectiveness of the criteria and their sensitivity in measuring the values

$\Delta_1 \div \Delta_4$ for vibration diagnostics of mechanical devices proposed by the authors based only on the example of the tested slide bearing.

After analysing the test results, it is possible to conclude that the RMS values (diagnostic criterion I_1 (2)) of the vibration acceleration of the bearing pan are parameters that can be used in the diagnosis of slide bearings as an indicator of correct bearing operation. The usefulness of time-frequency methods, in particular the Hilbert–Huang HHT method (diagnostic criterion I_4 (16)), has been demonstrated. This method is useful in relation to systems working in conditions of non-stationary and non-linearities of occurring phenomena. In the case of continuous operation of mechanical devices, especially drive devices, the proposed criteria can be used to detect emergency states. For the purposes of quantitative evaluation and comparison of the effectiveness of the diagnostic criteria, a sensitivity measure Δ_n (according to (18)) was defined for the change of vibration acceleration caused by the increasing load on the slide bearing. Analysis of the obtained results of the study (Tab. 2, Figs. 9–11) allows us to state that methods based on the determination of effective values (criterion I_1) and on HHT transformation (criterion I_4) of vibration acceleration in the bearing pan are characterised by higher values of the sensitivity measure Δ_n than methods based on Fourier transform (criterion I_2) or STFT transform (criterion I_3). It has also been shown that decrease of vibration acceleration values in one axis may be related to increase of vibrations in other axes. Therefore, in vibration diagnostics it is advisable to measure and analyse signals in a 3-axial system.

References

Borghesani P., Smith W.A., Zhang X., Feng P., Peng Z., 2018, *A new statistical model for acoustic emission signals generated from sliding contact in machine elements*, Tribology International, vol. 127, pp. 412–419. https://doi.org/10.1016/j.triboint.2018.06.032.

B&K, 2016, *Transducers and Conditioning*, Brüel & Kjær, https://www.bksv.com/-/media/literature/Catalogue/bf0236.ashx [access: 1.01.2016].

Cioch W., Knapik O., Leśkow J., 2013, *Finding a frequency signature for a cyclostationary signal with applications to wheel bearing diagnostics*, Mechanical Systems and Signal Processing, vol. 38, pp. 55–64. https://doi.org/10.1016/j.ymssp.2012.12.013.

Feldman M., 2011, *Hilbert Transform Applications in Mechanical Vibration*, John Wiley & Sons.

Gawędzki W., 2016, *Decomposition of mechanical vibration signals – the Hilbert–Huang Transform in the time domain and the Fourier Transform in the frequency domain*, Przegląd Elektrotechniczny, nr 11, pp. 69–72. https://doi.org/10.15199/48.2016.11.17.

Gawędzki W., Serzysko B., 2015, *Zastosowanie transformacji Hilbert Vibration Decomposition do analizy sygnałów parasejsmicznych w dziedzinie czasu*, Przegląd Elektrotechniczny, R. 91, nr 8, pp. 7–10. http://doi.org/10.15199/48.2015.08.02.

HBM, 2003, *Spider 8 User guide*, Hottinger Baldwin Messtechnik, https://www.hbm.com/fileadmin/mediapool/hbmdoc/technical/b0405.pdf.

Huang N.E., Shen Z., Long S.R., Wu M.C., Shih H.H., Zheng Q., Yen N.-C., Tung C.C., Liu H.H., 1998, *The empirical mode decomposition and the Hilbert spectrum for non-linear and non-stationary time series analysis*, Proceedings of the Royal Society of London. Series A: Mathematical, Physical and Engineering Sciences, vol. 454, pp. 903–995. https://doi.org/10.1098/rspa.1998.0193.

Lepiarczyk D., 2015, *Vibrothermography in diagnostic bearings during operation*, Vibroengineering PROCEDIA, vol. 6, pp. 145–149.

Lepiarczyk D., Gawędzki W., 2018, *Vibration Diagnostic of a Friction Process in Slide Bearings*, Tribologia, nr 2, pp. 73–80.

Obuchowski J., Wyłomańska A., Zimroz R., 2013, *Stochastic modelling of time series with application to local damage detection in rotating machinery*, Key Engineering Materials, vol. 569–570, pp. 441–448. https://doi.org/10.4028/www.scientific.net/KEM.569-570.441.

Obuchowski J., Wyłomańska A., Zimroz R., 2014a, *Selection of informative frequency band in local damage detection in rotating machinery*, Mechanical Systems and Signal Processing, vol. 48, pp. 138–152. https://doi.org/10.1016/j.ymssp.2014.03.011.

Obuchowski J., Wyłomańska A., Zimroz R., 2014b, *The local maxima method for enhancement of time-frequency map and its application to local damage detection in rotating machinery*, Mechanical Systems and Signal Processing, vol. 46, pp. 389–405. https://doi.org/10.1016/j.ymssp.2014.01.009.

Oppenheim A.V., Schafer R.W., Buck J.R., 1999, *Discrete-Time Signal Processing*, Prentice-Hall Signal Processing Series, Prentice Hall.

Poddar S., Tandon N., 2019, *Detection of particle contamination in journal bearing using acoustic emission and vibration monitoring techniques*, Tribology International, vol. 134, pp. 154–164. https://doi.org/10.1016/j.triboint.2019.01.050.

Poulimenos A.G., Fassois S.D., 2006, *Parametric time-domain methods for non-stationary vibration modelling and analysis – A critical survey and comparison*, Mechanical Systems and Signal Processing, vol. 20, pp. 763–816. https://doi.org/10.1016/j.ymssp.2005.10.003.

Tse P.W., Yang W.X., Tam H.Y., 2004, *Machine fault diagnosis through an effective exact wavelet analysis*, Journal of Sound and Vibration, vol. 277(4–5), pp. 1005–1024. https://doi.org/10.1016/j.jsv.2003.09.031.

Turowicz A., 2005, *Teoria macierzy*, Uczelniane Wydawnictwa Naukowo-Dydaktyczne AGH, Kraków.

Wyłomańska A., Obuchowski J., Zimroz R., Hurd H., 2014, *Periodic autoregressive modelling of vibration time series from planetary gearbox used in bucket wheel excavator*, [in:] Chaari F., Leśkow J., Napolitano A., Sanchez-Ramirez A. (eds.), *Cyclostationarity: Theory and Methods*, Lecture Notes in Mechanical Engineering, Springer, Cham, pp. 171–186. https://doi.org/10.1007/978-3-319-04187-2_12.

Yang B.S., Kim K.J., 2006, *Application of Dempster–Shafer theory in fault diagnosis of induction motors using vibration and current signals*, Mechanical Systems and Signal Processing, vol. 20, pp. 403–420. https://doi.org/10.1016/j.ymssp.2004.10.010.